#7462

Journal of Wind Engineering and Industrial Aerodynamics, 46 & 47 (1993) 95–104
Elsevier

Influence of the Turbulence Model in Calculations of Flow over Obstacles with Second-Moment Closures

A. O. DEMUREN
Associate Professor, Department of Mechanical Engineering and Mechanics, Old Dominion University, Norfolk, VA 23529, U.S.A.

Abstract

This paper investigates the role of turbulence models in numerical calculations of flow over obstacles with second-moment closure models. Two models for the pressure-strain correlations are examined in the study. Computations of the main characteristics of the mean flow and the turbulent fields are compared against experimental data, and results obtained with the standard k-ϵ model. All models give reasonable agreement with the data. In the limited region in which comparisons were made, the k-ϵ model gives the best agreement with mean flow data, and the LRR model gives better agreement with Reynolds stress data.

1. INTRODUCTION

The flow over obstacles is encountered in many engineering applications in internal or external environments. This paper explores the role of the turbulence model in calculations of two-dimensional flow over a rectangular obstacle in a channel. A recent study of second-moment closure models by Demuren and Sarkar[1] has shown significant influence of the model for the pressure-strain correlation on the distribution of Reynolds stresses in plane channel flows. The most successful models in that study were those due to Launder, Reece and Rodi[2] (denoted LRR), and Speziale, Sarkar and Gatski[3] (denoted SSG). The latter has the advantage that it could reproduce correctly variations in Reynolds stress anisotropies between the log-layer and the core near the center of the channel without any special wall-proximity modifications, whereas the former required wall reflections terms to achieve this. Both models are utilized in the present study, and computed results are compared to those with the standard k-ϵ turbulence model and experimental data of Dimaczek et al. [4]. In [1], three models for approximating the turbulent diffusion terms in the Reynolds stress equations were examined. These are based on proposals by Daly and Harlow[5] (denoted DH), Hanjalic and Launder[6] (denoted HL), and Mellor and Herring[7] (denoted MH). It was found that only the MH model enabled the reproduction of the experimentally observed relaxation towards isotropy near the center of the channel. Hence, the MH model is utilized in the present study.

In previous computational studies of the present flow situation, Kessler et al.[8] used the standard k-ϵ model and Obi et al.[9] used a simpler version of the LRR pressure-strain model along with the DH diffusion model. In both studies, rectangular grids were utilized, with the region containing the obstacle blocked off. In contrast, curvilinear, body-fitted grids (see Fig. 1) are utilized in the present study. This simplifies considerably the implementation of a multigrid procedure and has the advantage that grid lines are more aligned with the flow thereby minimizing artificial diffusion. On the other hand, discretization errors may be increased in regions with rapid changes in grid curvature. These are confined to the corner regions.

2. MATHEMATICAL FORMULATION

2.1 Mean Flow Equations

The Reynolds-averaged mean-flow equations for steady, incompressible turbulent flow can be written in Cartesian tensor notation as:

Continuity

$$\frac{\partial}{\partial x_i}\left(|J| U_m \alpha^i_m\right) = 0 \tag{1}$$

Momentum

$$\frac{\partial}{\partial x_l}\left(|J| U_m U_i \alpha^l_m\right) = -\frac{1}{\rho}\frac{\partial}{\partial x_l}\left\{|J|\left[P\delta_{mi} + \rho\overline{u_i u_l} - \mu\left(\frac{\partial U_i}{\partial x_n}\alpha^n_m + \frac{\partial U_m}{\partial x_k}\alpha^k_l\right)\right]\alpha^l_m\right\} \tag{2}$$

where $x_i=(x_1, x_2, x_3)$ represent the curvilinear coordinates, related to the Cartesian coordinate system (y_1, y_2, y_3) by the transformation $y_j = y_j(x_i)$. $|J|$ is the Jacobian of the transformation. The metrics $\alpha^i{}_j$ are elements of the Jacobian of the inverse transformation $x_i = x_i(y_j)$, and δ_{mi} is the Kronecker delta. (U_1,U_2,U_3) are Cartesian mean velocity components, P is the pressure, μ the molecular viscosity and ρ the density. Einstein's summation rule for repeated indices is utilized. $\overline{u_i u_l}$ (with i=1,2,3, and l=1,2,3) represents the six components of the Reynolds stress tensor, R_{il} which must be determined by the turbulence model. In the two-dimensional flow, with walls in the (1–3) and (2–3) planes, $\frac{\partial}{\partial x_3} = 0$ in equations (1) and (2), and R_{il} will have only 4 non-zero components; the three diagonal elements $\overline{u_1^2}$, $\overline{u_2^2}$ and $\overline{u_3^2}$ which represent the normal stresses, and one off-diagonal element $\overline{u_1 u_2}$ which represents the shear stress.

2.2 Reynolds Stress Equations

The transport equations for the Reynolds stress components can be written for high Reynolds number turbulent flow in Cartesian tensor notation as:

$$\frac{\partial}{\partial x_l}\left(|J|U_m\overline{u_i u_j}\alpha_m^l\right) = |J|(D_{ij} + P_{ij} + \pi_{ij} - \epsilon_{ij}) \tag{3}$$

where D_{ij} is the diffusion, P_{ij} is the production, π_{ij} is the pressure-strain correlation, and ϵ_{ij} is the dissipation rate.

The production term is $P_{ij} = -\overline{u_i u_l}\frac{\partial U_j}{\partial x_m}\alpha_l^m - \overline{u_j u_l}\frac{\partial U_i}{\partial x_m}\alpha_l^m$; and the dissipation is assumed to be locally isotropic so that $\epsilon_{ij} = 2/3\ \delta_{ij}\epsilon$, where ϵ is the dissipation rate of the turbulent kinetic energy k, to be determined from the solution of a transport equation.

The MH model gives D_{ij} as

$$D_{ij} = 0.072\frac{k^2}{\epsilon}\left[\frac{\partial\overline{u_i u_j}}{\partial x_m}\alpha_k^m + \frac{\partial\overline{u_i u_k}}{\partial x_m}\alpha_j^m + \frac{\partial\overline{u_j u_k}}{\partial x_m}\alpha_i^m\right] \tag{4}$$

This is a gradient diffusion model with isotropic coefficient. The symmetry in the indices ijk is preserved, unlike in the more popular DH model.

2.3 Pressure-Strain Models

By far the most popular approximations for the pressure-strain correlation are the two LRR models. Although the simpler version (model 2), based on the isotropization of production, is more widely used in complex flow applications, the quasi-isotropy version (model 1) is preferred for channel flow computations because it produces the correct level of the anisotropy in Reynolds stresses, in the equilibrium log-layer. It also has a form which is closer to those of newer, more complex, pressure-strain models. In their model 1, LRR proposed to account for wall-proximity effects by making coefficients in the expressions functions of the average distance from walls. In model 2, usually called the Gibson-Launder model, they are treated as wall-reflection terms. These wall-reflection terms are not near-wall corrections in the conventional sense, since they are applicable to the fully turbulent region beyond the viscous sublayer and the buffer zone, and they still have significant contributions at the center of the channel. However, there is uncertainty as to how rapidly the functions should decay with distance from walls, and in flows with corners or with complex geometries the treatment of wall reflection terms may become ambiguous. For example, in the computations of Obi et al.[9], these terms were simply set to zero at distances beyond 100 wall units. Hence, it is now generally accepted that the need for special wall-proximity treatment is an undesirable feature in a pressure-strain model. Recently, Speziale, Sarkar and Gatski[8] (denoted SSG) proposed a model for the pressure-strain correlation based on an invariant dynamical-systems approach. The model was calibrated with results from experimental and theoretical studies of homogeneous and rotating homogeneous shear flows. The resulting model appears to be only slightly more complex than the quasi-isotropy model of LRR. Demuren and Sarkar [1] have found that the SSG model could predict the Reynolds stress anisotropy levels in developed channel flow without the use of any wall reflection terms, at least as well as the LRR model with wall reflection terms. This is a desirable quality and it is of interest to compare the performance of both the LRR and SSG models.

The pressure-strain models can be written in terms of the anisotropy tensor $b_{ij} \equiv (\overline{u_i u_j}/2k - \frac{1}{3}\delta_{ij})$, the rate of strain tensor $S_{ij} \equiv \frac{1}{2}\left(\frac{\partial U_i}{\partial x_m}\alpha_j^m + \frac{\partial U_j}{\partial x_m}\alpha_i^m\right)$, the rotation tensor $W_{ij} \equiv \frac{1}{2}\left(\frac{\partial U_i}{\partial x_m}\alpha_j^m - \frac{\partial U_j}{\partial x_m}\alpha_i^m\right)$, and the rate of production of turbulent kinetic energy P_k in the general form :

$$\begin{aligned}\pi_{ij} = \; & \alpha_0 \epsilon b_{ij} + \alpha_1 \epsilon (b_{ik} b_{jk} - 1/3 II \delta_{ij}) + \alpha_2 k S_{ij} + \alpha_3 P_k b_{ij} + \\ & + k\{\alpha_4 (b_{ik} S_{jk} + b_{jk} S_{ik} - 2/3 \delta_{ij} b_{kl} S_{kl}) + \alpha_5 (b_{ik} W_{jk} + b_{jk} W_{ik})\}\end{aligned} \tag{5}$$

The model coefficients $\alpha_0 \ldots \alpha_5$ may be, in general, functions of the invariants of the anisotropy tensor. The corresponding relations for the two pressure-strain models are $\alpha_0 = -(3.0 - f); \alpha_1 = 0; \alpha_2 = 0.8; \alpha_3 = 0; \alpha_4 = 1.745; \alpha_5 = 1.309 - 0.24f$: for the LRR model, and $\alpha_0 = -3.4; \alpha_1 = 4.2; \alpha_2 = 0.8 - 1.3 II^{1/2}; \alpha_3 = -1.8; \alpha_4 = 1.25; \alpha_5 = 0.4$: for the SSG model. $f = \left(\frac{c_\mu^{3/4}}{\kappa n}\frac{k^{3/2}}{\epsilon}\right)^2$ is the wall-proximity function. n is calculated in this study as the shortest distance to any wall. $II = b_{lk}\, b_{kl}$ is the second invariant of the Reynolds stress anisotropy tensor.

2.4 k-ϵ Model

Calculations were also made with the standard high-Reynolds number form of the k-ϵ turbulence model. The equations for k and ϵ can be expressed in tensor notation as:

$$\frac{\partial}{\partial x_l}\left(|J| U_m k \alpha_m^l\right) = \frac{c_\mu}{\sigma_k}\frac{\partial}{\partial x_l}\left\{\left[|J|\frac{k^2}{\epsilon}\left(\frac{\partial k}{\partial x_n}\alpha_m^n\right)\right]\alpha_m^l\right\} + |J|(P_k - \epsilon) \tag{6}$$

$$\frac{\partial}{\partial x_l}\left(|J| U_m \epsilon \alpha_m^l\right) = \frac{c_\mu}{\sigma_\epsilon}\frac{\partial}{\partial x_l}\left\{\left[|J|\frac{k^2}{\epsilon}\left(\frac{\partial \epsilon}{\partial x_n}\alpha_m^n\right)\right]\alpha_m^l\right\} + |J|\left(c_{\epsilon 1}\frac{\epsilon}{k}P_k - c_{\epsilon 2}\frac{\epsilon^2}{k}\right) \tag{7}$$

This standard form of the ϵ equation is also used to close the Reynolds stress equations. This deviates somewhat from the common practice in the literature in which anisotropic diffusion coefficients are used which depend on the Reynolds stress anisotropies. Equation (7) avoids this dependency and should enable the role of the pressure-strain model to be better isolated. The empirical constants are : $\sigma_k = 1.0$; $\sigma_\epsilon = 1.3$; $c_{\epsilon 1} = 1.44$; $c_{\epsilon 2} = 1.92$; $c_\mu = 0.09$; $\kappa = 0.40$.

2.5 Solution Procedure

The set of equations is solved by a two-dimensional, finite volume, numerical procedure which uses a non-linear multigrid method to accelerate the convergence. This follows closely the three-dimensional finite-volume method described in detail by Demuren[10]. On the coarsest level, 27 by 10 grid points are used in the (x_1,x_2) directions as shown in Fig. 1 (a). All variables are stored at the center of the cell in a non-staggered arrangement. Finer grids are generated by halving each side. A 4-level multigrid scheme is utilized for the finest grid which has 210 by 74 points. The distribution in the vicinity of the block is shown in Fig. 1 (b). On this grid convergence to a normalized residual norm of 10^{-3} required about 450 fine grid iterations and a total of 720 work units at a cost of 480 CPU seconds on the CRAY YMP computer, when the k-ϵ model was utilized, and 780 fine grid iterations, 1200 total work units and 3000 CPU seconds when the Reynolds stress models were utilized. Better convergence rates could probably be obtained with optimization of the procedure.

The objective of this work is to compare the behavior of established turbulence models, so computations are for the high Reynolds number flow region only, in which the viscous sublayer is not resolved but is bridged using the standard wall-function method. Flow separation along the lower wall calls into question the appropriateness of standard wall-function method. To alleviate the difficulties which occur when U_τ goes to zero at the point of separation it is replaced by $c_\mu^{1/4}k^{1/2}$ in the log-law, following Obi et al.[9]. Along the line of nodes nearest to the walls, local equilibrium is assumed: $k = U_\tau{}^2/c_\mu{}^{1/2}$; $\epsilon = U_\tau{}^3/(\kappa n)$; and in the horizontal direction, $\overline{u_1^2} = 1.07\,k$; $\overline{u_2^2} = 0.41\,k$; $\overline{u_3^2} = 0.52\,k$; $\overline{u_1u_2} = -0.30\,k$. The values for $\overline{u_1^2}$ and $\overline{u_2^2}$ are transposed in the vertical direction, and interpolated using cosine functions for grid lines which lie in between. Inlet conditions are derived from computed results for a fully-developed plane channel flow at a Reynolds number (based on mean velocity and channel height) of 10^5, using the SSG model.

3. RESULTS AND DISCUSION

Predictions of the mean streamwise velocity and the turbulent kinetic energy at two locations downstream of the block are compared with experimental data [4] in Fig. 2. Similar to findings of Obi et al. [9], the prediction of the mean flow obtained with the k-ϵ model agrees better with the data than those obtained with the Reynolds stress models. Both Reynolds stress models give similar predictions of the mean flow. Experimental data give the length of the recirculation zone behind the block as 7.1 block heights. The computations with the k-ϵ, LRR, and the SSG models give the length as 6.6, 6.7, and 7.3 heights, respectively. These are all within the range of the experimental uncertainty. Mean flow results are relatively grid independent, since computed results on third- and fourth-level grids indicated changes in the peak cross-sectional velocity and the recirculation length which were less than 2 %. However, peak values of k showed larger changes, so predicted turbulence fields may not be grid independent, and the discussion below is made with this reservation.

Figure 2 shows that the k-ϵ model gives k values which agree quite well with the data at $y_1/H=5$, but are underpredicted at $y_1/H=9$. Both the LRR and the SSG models underpredict k at $y_1/H=5$, but the LRR model gives the correct maximum value at $y_1/H=9$, although not at the right location. The SSG model still underpredicts k at the latter location. These results agree with findings of Demuren and Sarkar[11] in plane mixing layer computations, in which it was found that only the LRR model predicted the correct maximum turbulence intensity level. Both the SSG model and the k-ϵ model underpredicted it.

Predicted Reynolds stresses are compared in Figs. 3 and 4. Neither model gives perfect agreement with the data, but on the average, the LRR model appears to perform better. Clearly, the underprediction of k by the SSG model shows up in the distribution amongst its components. Present predictions with the LRR model agree somewhat better with experimental data than results presented by Obi et al. [9]. This could be due to differences in the form of the model, the grid distribution, or in the inlet conditions. A surprising observation is that the experimental data indicate very little anisotropy in the Reynolds stresses. For example, at $y_1/H=5$, almost perfect agreement is obtained (not shown) by splitting the k values equally into its three components, i.e., assuming complete isotropy. This level of isotropy is not obtained with either Reynolds stress model. The mechanism for producing this in the experiment is not clear at this time. Clearly, plane channel flows and plane mixing layers, which may be combined to synthesize the present flow are highly anisotropic. Further investigation is needed to explain this. Perhaps, new results from large eddy simulation will provide some answers.

4. CONCLUDING REMARKS

Computations of two-dimensional turbulent flow over a rectangular block placed in a channel were made with two Reynolds stress models and the standard high-Reynolds number turbulence k-ϵ model. The k-ϵ model results agree reasonably well with the data in the region, beyond two heights behind the block, investigated in detail. The Reynolds stress models give reasonable, but not perfect agreement with the data in this region. On the average, the LRR model seems to perform better.

5. ACKNOWLEDGMENT

The computations were performed on the Cray YMP computer of the NAS program at NASA Ames Research Center, Moffet Field, California.

6. REFERENCES

1. Demuren, A.O., and Sarkar, S., ICASE Report No. 92–19, 1992.
2. Launder, B.E., Reece, G.J., and Rodi, W., J. Fluid Mech., Vol. 68, 1975, pp. 537–566.
3. Speziale, C.G., Sarkar, S. and Gatski, T.B., J. Fluid Mech., Vol. 227, 1991, pp. 245–272.
4. Dimaczek, G., Kessler, R., Martinuzzi, R. and Tropea, C., Proc., Seventh Symp. Turbulent Shear Flow, Stanford, California, 1989, pp. 10.1.1–10.1.6.
5. Daly, B.J. and Harlow, F.H., Phys. Fluids, Vol. B, 1970, pp. 2634–2649
6. Hanjalic, K., and Launder, B.E., J. Fluid Mech., Vol. 52, 1972, pp. 609–638
7. Mellor, G.L., and Herring, H.J., AIAA J., Vol. 11, 1973, pp. 590–599.

8. Kessler, R., Peric, M., and Scheuerer, G., AGARD Conf. Proc. No. 437, 1988, pp. 9.1–9.12.
9. Obi, S., Peric, M., and Scheuerer, G., Proc., Int. Symp. on Engg. Turb. Model. and Measur., Dubrovnik, Yugoslavia, 1990.
10. Demuren, A.O., “Multigrid Acceleration and Turbulence Models for Computations of 3D Turbulent Jets in Crossflow,” Int. J. Heat Mass Trans., 1992, (in press).
11. Demuren, A.O., and Sarkar, S., “Study of Second-Moment Closure Models in Computations of Turbulent Shear Flows”, Proc., 2nd. Int. Symp. on Engg. Turb. Model. and Measur., Florence, Italy, 1993.

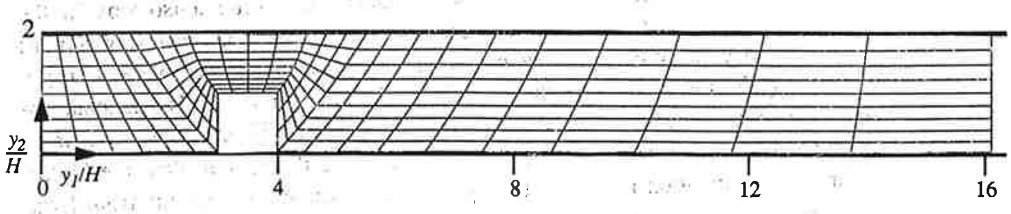

(a) coarsest grid

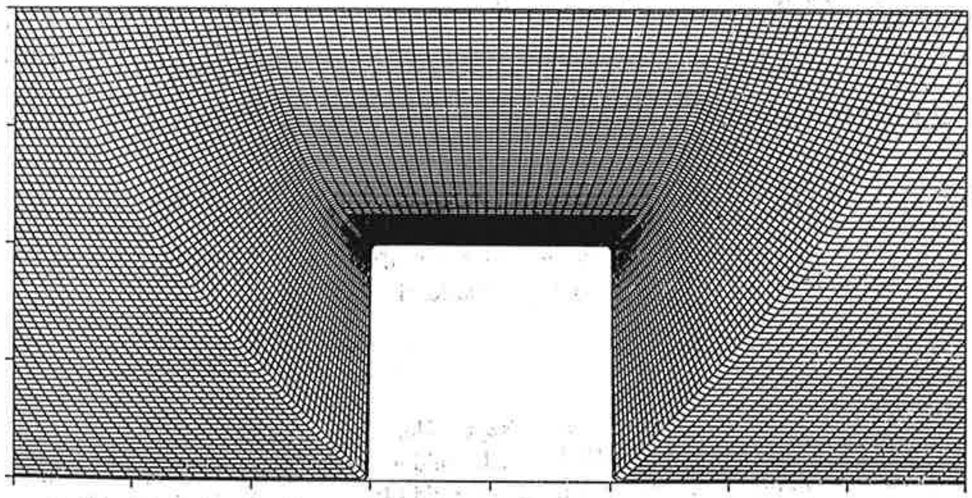

(b) finest grid

FIGURE 1. Flow configuration and computational grids.

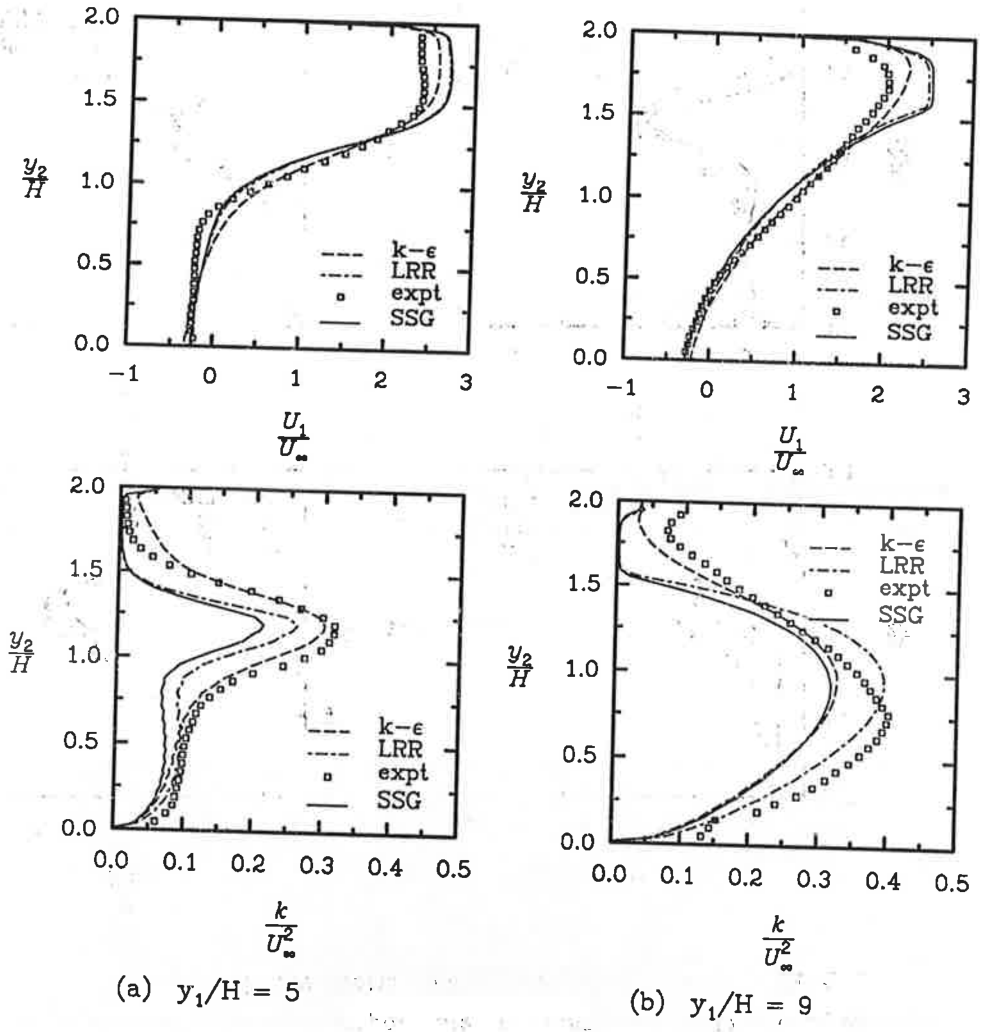

FIGURE 2. Comparison of RSM and k−ε results with experimental data of Dimaczek et al.[4], at y_1=5H & 9H.

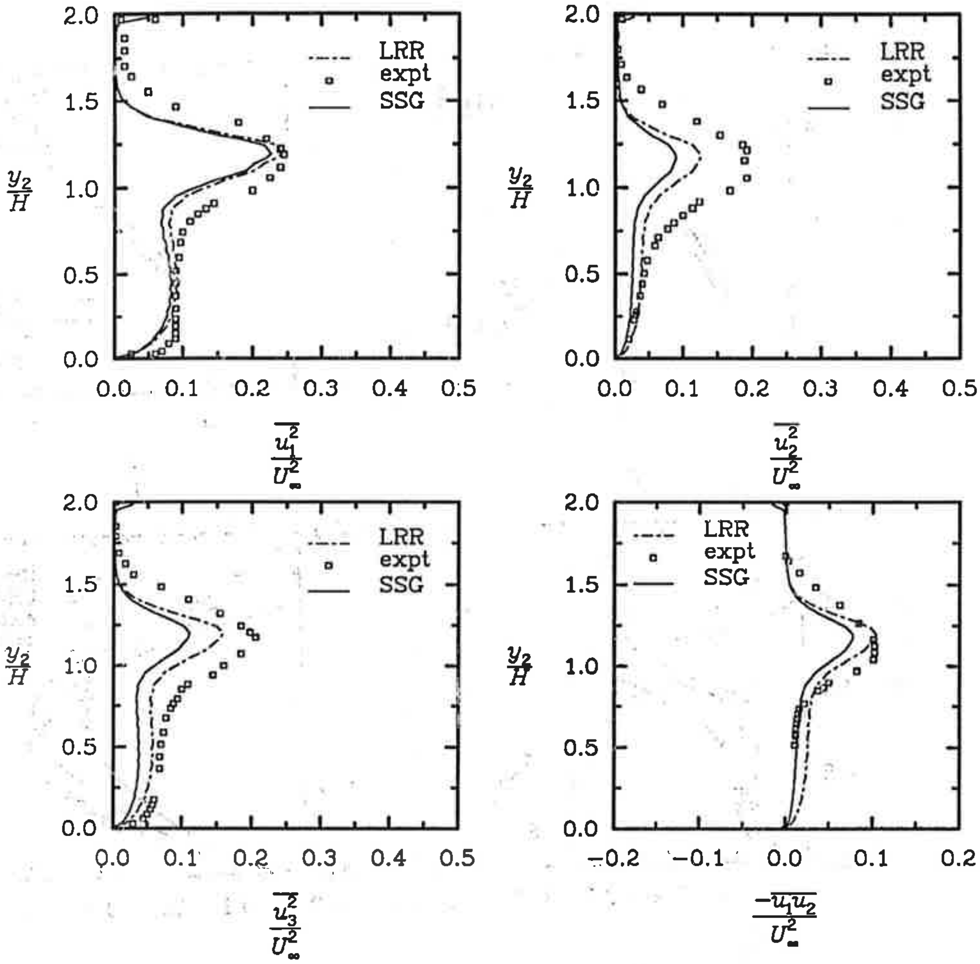

FIGURE 3. Comparison of Reynolds stresses at y_1=5H: Influence of the pressure−strain model.

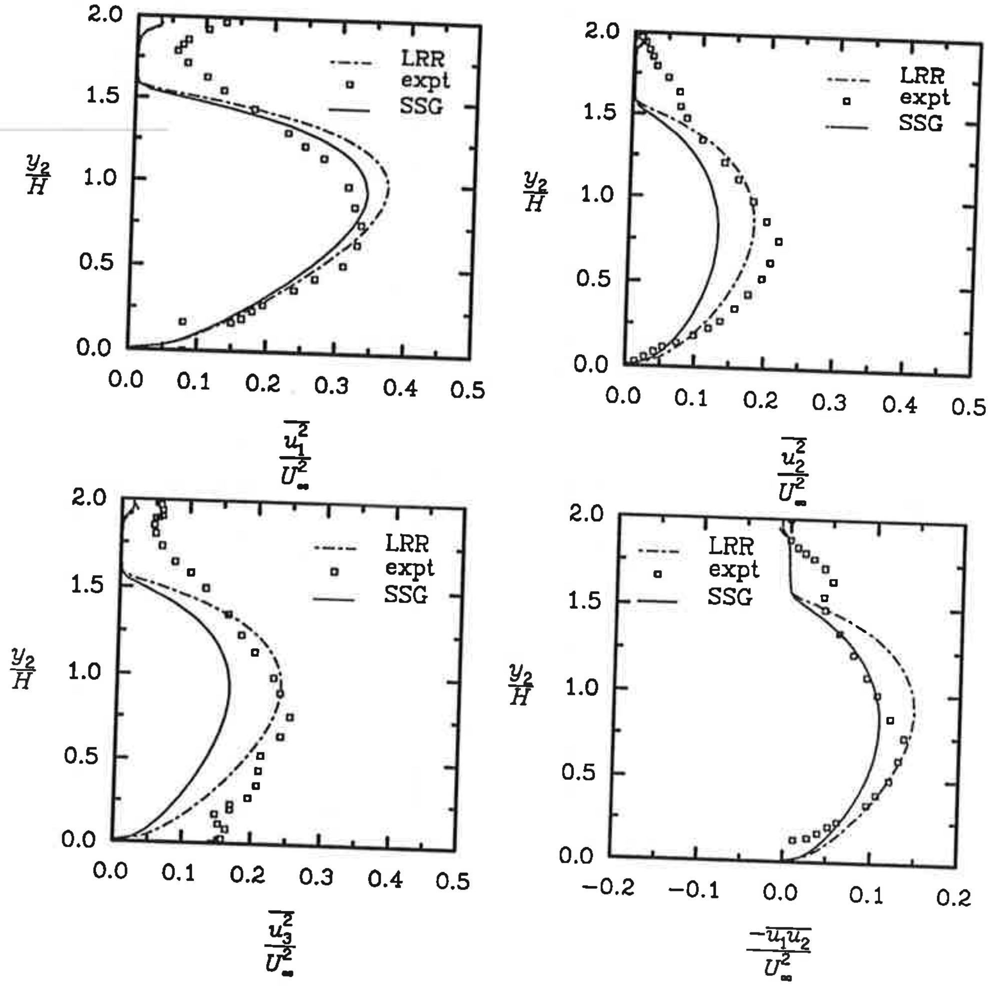

FIGURE 4. Comparison of Reynolds stresses at y_1=9H: Influence of the pressure−strain model.